Journal of Materials Processing Technology 213 (2013) 1327–1336

Contents lists available at SciVerse ScienceDirect

Journal of Materials Processing Technology

journal homepage: www.elsevier.com/locate/jmatprotec

# Electro-thermal measurements and finite element method simulations of a spark plasma sintering device

A. Pavia[a,b], L. Durand[b,c], F. Ajustron[b,c], V. Bley[b,d], G. Chevallier[a], A. Peigney[a,b], C. Estournès[a,b,*]

[a] CNRS, Institute Carnot Cirimat, F-31602 Toulouse cedex 9, France
[b] Université de Toulouse, Institut Carnot CIRIMAT, UPS CNRS, Université Paul-Sabatier, 31062 Toulouse cedex 9, France
[c] CNRS – CEMES (Centre d'Elaboration de Matériaux et d'Etudes Structurales), Toulouse, France
[d] LAPLACE, Toulouse, France

ARTICLE INFO

Article history:
Received 30 October 2012
Received in revised form 28 January 2013
Accepted 2 February 2013
Available online xxx

Keywords:
SPS
Thermal and electrical measurement
Modeling, FEM

ABSTRACT

Current, voltage and temperature measurements were performed at different points of the system to identify the controlling parameters of the spark plasma sintering (SPS) process. The very low inductance effects despite the high intensity current circulating through the SPS column justifies the use of Joule heating to characterize the phenomenon. The measurements also enabled the improvement and validation of an earlier electro-thermal numerical model developed using the finite element method (FEM). It has been shown that the electrical resistivity and the thermal conductivity of each of the elements are crucial parameters for the simulations. These parameters strongly modify the current modeled, thereby affecting the temperature distribution throughout the SPS column.



## 1. Introduction

SPS (Spark Plasma Sintering) which consists of heating by applying a pulsed direct current through the die, and sometimes through the sample, while applying a uniaxial pressure allows high consolidation and densification rates with negligible grain growth (Chaim et al., 2008). But, many questions still remain concerning both the mechanisms involved and the electrical and thermal behavior of the tools during the SPS cycles. In particular few studies have been performed on the influence of the pulse sequences of the current generated by the SPS machines on the temperature distribution in the tools. Cincotti et al. (2007) developed electrical instrumentation on a 515S SPS apparatus (Sumitomo Heavy Industries Ltd., Kanagawa, Japan) to measure the current and voltage with a high sampling frequency. They determined the root mean square values (RMS) of this recording in order to simulate the distributions of temperature, current and strain in the SPS graphite stack containing no sample. Several measurements and models highlight the presence of temperature gradients depending on the electrical properties (conductivity) of the samples to be sintered. Wang et al. (2010) also carried out a FEM simulation of temperature and stress distributions in an SPS Stack containing an insulating sample (i.e.: alumina). Their FEM analysis includes a self-defined Proportional-Integral-Differential (PID) Module which is able to control the temperature and heating rates along the SPS cycle. Munoz and Anselmi-Tamburini (2010) also used a simulation code that includes a PID Module to compare the modeled temperature and stress field distributions in the SPS stack containing either a conducting material (copper) or an insulating material (alumina). A common view of these authors is that current distribution is an important factor in the distribution of temperatures within the equipment. The determination of the RMS values of the voltage ($U_{RMS}$) across and the current ($I_{RMS}$) passing through the SPS tools, the latter being responsible for its heating by Joule effect, is essential to evaluate the thermal gradients in the SPS column.

In this study a specific instrumentation has been developed to perform simultaneous temperature measurements at several points of the SPS column and electrical measurements across it, giving real time thermal and electrical conditions of the stack during the overall sintering cycle the (Fig. 1). Then, the different values collected were used as input data to an SPS numerical model of electro-thermal coupling already developed by some of the authors: Molénat et al. (2010). Finally, the model was improved with the results obtained.

## 2. Electrical and thermal measurements

### 2.1. Experimental

#### 2.1.1. Electrical measurements: measurements of the RMS values

In usual SPS machines, the input source to heat the tools is a pulsed direct current for which the waveform pattern can vary.

* Corresponding author at: CIRIMAT 118, route de Narbonne 31062, Toulouse, France. Tel.: +33 561556109; fax: +33 561556163.
E-mail address: estournes@chimie.ups-tlse.fr (C. Estournès).

0924-0136/$ – see front matter 
http://dx.doi.org/10.1016/j.jmatprotec.2013.02.003

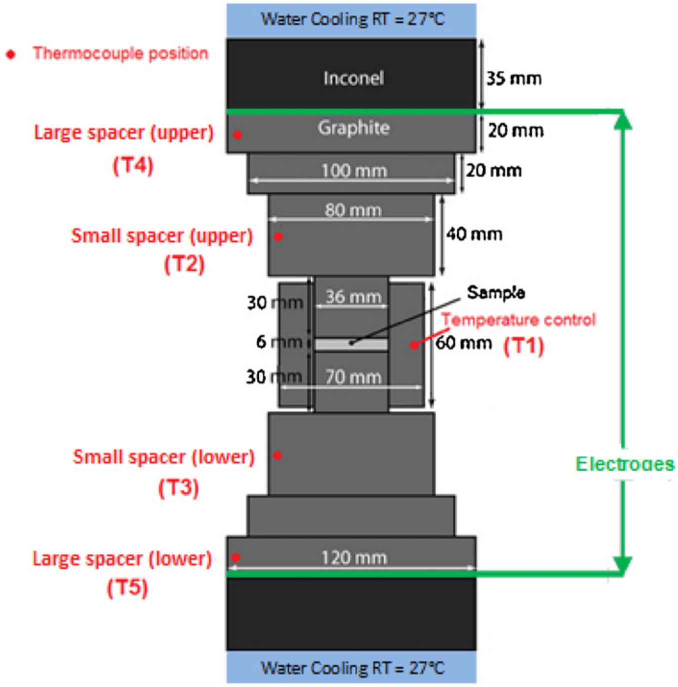


**Fig. 1.** Diagram of the SPS: dimensions of each element, position of thermocouples and water cooling.

Industrial SPS devices are equipped with current and voltage sensors which provide average values (of the magneto-electric type) all along the sintering cycles. These data are crucial to determining the power injected into the device for resistive heating. This electrical power $P$ dissipated in a heater of resistance $R$ and transformed into heat is expressed by Joule's law (1):

$$P = \frac{1}{T}\int_{t-T}^{t} u(\tau)i(\tau)d\tau = \frac{R}{T}\int_{t-T}^{t} i^2(\tau)d\tau \quad (1)$$

where $u$ and $i$ are the instantaneous voltage and current applied to the sample and $T$ the AC period.

This relation is valid for direct currents (voltages) (without an AC component) as well as alternative currents (voltages) but in this later case $U$ and $I$ represent the RMS values. In addition, this relation is no longer valid if the circuit contains a reactive component, the dipole considered should be purely resistive. In most SPS devices, the current delivered is not a pure DC current an alternating component is present, so the common configuration (12 current pulses and two timeouts), is a quasi-periodic pulsed DC current. To allow power modulation, the three-phase full-wave rectification pulses were individually controlled by delaying the initiation of the silicon-controlled rectifier (SCR). The pulse characteristics were variable depending on the power required by the PID temperature controller to satisfy the set-point temperature. So, the current was not sinusoidal, the RMS current and voltage should be calculated for a whole number of periods. The relationship to obtain the RMS voltage is of the form (2):

$$U_{\text{RMS}} = \sqrt{\frac{1}{T}\int_{t-T}^{t} u^2(\tau)d\tau} \quad (2)$$

The RMS intensity of the current is given by a similar expression. Thus, to evaluate the power dissipated in the heating tools, the RMS values of the voltage and the intensity of the current should be determined. To do so, specific instrumentation was developed.

When confronted with a pulsed current, instantaneous magnitudes of $u(t)$ and $i(t)$ must be recorded to calculate their RMS values. To do so, sensors were selected for sampling the signals ($u(t)$ across the column and $i(t)$ passing through) with a sufficiently high frequency (up to 10,000 Hz) to describe each pulse correctly. The intensity of current delivered by the SPS machine (SPS Syntex Inc., model 2080) used in this study can be as high as 8000A. For security reasons and accuracy of the measurements, it is important to not modify this high power circuit and to achieve current measurements without contact. Ray and Davis (1999) have shown that a wide band Rogowski coil sensor (Power Electronic Measurements, CWT60) can be used for measuring current at high frequency bandwidths up to 7 MHz. Ray (1999) stated that this probe also allows the measurement of high level pulsed currents. However, one of the limits of this type of sensor is that it is not able to measure the DC component of a current, which corresponds to its average value. Therefore, using this type of sensor, the DC component of the signal should be restored prior to the calculation of its average and effective values. Fortunately, this becomes possible by correcting it from the values measured at the dead times where it should be null. From the instantaneous voltage and intensity measurements, average and RMS values are calculated using a Labview routine (National Instrument software). The signal was also calibrated using an oscilloscope to verify the correspondence between measured and calculated mean values. To measure the voltage across the SPS column, the potential was considered uniform over the entire contact surface. To improve the voltage measurement accuracy, stainless steel electrodes were designed to be placed directly between the large upper graphite spacer and the Inconel part (Fig. 1). These electrodes were linked to a differential input of the NI Compact DaQ system.

### 2.1.2. *Temperature measurements*

A set-up equipped with 8 K-type thermocouples was also developed in order to perform temperature measurements at several points of the column at the same time as electric data acquisition. The data collected were synchronized with the electrical measurements using a Labview routine. The data files thus generated were used to feed the model developed or to validate it. The thermocouple positions are indicated in Fig. 1; T1 control temperature at the surface of the graphite die, T2 and T3 (upper and lower respectively) temperatures on the small spacers, T4 and T5 (upper and lower respectively) temperatures on the large spacers.

### 2.1.3. *Standard SPS experiments*

To achieve electro-thermal modeling of the SPS system as faithfully as possible while limiting approximations, standard experiments have been defined. These SPS manipulations were performed on graphite dies of 36 mm inner diameter and on conducting (manganese) and non-conducting (alumina) samples of 6 mm thickness. The samples were previously compacted to get rid of any changes in their densities because porosity has a strong influence on their physical properties. An experiment without a sample (graphite against graphite) was also conducted. The thermal cycle studied consisted of a rise in temperature at 100 °C/min up to 900 °C with a dwell time of 5 min at this temperature. A pressure of 100 MPa is applied from room temperature to minimize the electrical contact resistances.

## 2.2. *Results and discussions*

From the thermal data, when comparing the temperature measurements of the upper and lower large spacers, that the graphite parts located below the matrix were found warmer than that located above. Even if the column seems to be geometrically symmetrical, it does not seem to be in terms of heat transfer. This may be due to the non-symmetry of heat loss by radiation, but more likely to the non-symmetry of heat loss through conducto-convection at